

Excess thermodynamic and elastic properties of mineral and melt solutions: modelling and implications for phase relations and seismic velocities

R. Myhill

Bayerisches Geoinstitut, Universität Bayreuth, Universitätsstrasse 30, 95447 Bayreuth, Germany

Abstract

Thermodynamic models of solid and liquid solutions in the Earth Sciences are increasingly used to calculate phase relations and seismic properties over large pressure and temperature ranges. Research into mantle phase relations, subduction and differentiation of the early Earth frequently involves calculations spanning thousands of Kelvin and tens of gigapascals. Over such huge ranges, excess entropy and volume are unlikely to remain constant with respect to pressure and temperature, as is often assumed in solution models. In particular, absolute excess volumes tend to decrease with increasing pressure. The implication is that to provide a good estimate of phase relations and seismic velocities, solution models must be flexible enough to accommodate changes in elastic and thermodynamic derivatives, such as the bulk modulus.

This paper describes an extension to the subregular Margules mixing model which employs intermediate compounds to define the excess thermodynamic properties of solid solutions. Mathematical derivations are provided for excess thermodynamic properties (enthalpy, entropy, volume) and their pressure and temperature derivatives (bulk modulus, thermal expansion etc.). Heuristics are suggested for intermediate compounds where individual thermodynamic properties are poorly constrained.

*Corresponding author: R. Myhill
Email address: myhill.bob@gmail.com (R. Myhill)

Examples of pyroxene, garnet and melt solutions show that accurate modelling of phase relations and seismic velocities requires absolute excess volumes to decrease as a function of pressure. The magnitude of the excess volume and negative excess bulk modulus in these systems are strongly correlated. The formulation proposed here allows for a wealth of experimental data to be incorporated into solution models, and is expected to be important for geochemical and geophysical models of the Earth and other planetary bodies.

Keywords: high pressure, excess properties, solution model, solid, melt, elasticity

1. Introduction

Solution models are a vital part of estimating phase relations at high pressure and temperatures. Typically, experimental estimates of excess Gibbs free energy across a binary solution are fit to some functional form (often quadratic, cubic).

- 5 The variables for these functions are called interaction parameters, and generally have the form

$$W_{ij}^{\mathcal{G}} = W_{ij}^{\mathcal{H}} + W_{ij}^{\mathcal{V}}P + W_{ij}^{\mathcal{S}}T \quad (1)$$

- The enthalpic \mathcal{H} , entropic \mathcal{S} and volumetric \mathcal{V} contributions to each parameter can be derived from calorimetry, phase relations and X ray diffraction. These models have been extremely successful in describing the thermodynamic
- 10 properties of solid solutions at crustal pressures and temperatures. Under such conditions, the linear pressure and temperature approximation in Equation 1 is perfectly reasonable, as deviations from constant volume and entropy excesses are small. However, thermodynamic models are now being extended over much larger pressure and temperature ranges (Stixrude and Lithgow-Bertelloni, 2011;
- 15 Holland and Powell, 2011; Holland et al., 2013; de Koker et al., 2013). It is unlikely that excess properties will remain constant over these ranges. For example, imagine two crystal lattices (A_xO_y and B_xO_y) comprising cations with different ionic radii and field strengths. The properties of the cations (and anion) result in different unit cell volumes and compressibilities; typically the

20 lattice with the larger cationic radius will have a large volume and smaller bulk
 modulus (Anderson and Anderson, 1970). Now imagine a third lattice with
 intermediate composition ($[A_{1-z}B_z]_xO_y$). This lattice will typically exhibit dis-
 tortions which result in a positive or negative excess volume, as a direct result
 of changing the average cation-anion bond length relative to the sum of the end-
 25 members (Vegard’s Law). It is reasonable to suggest that longer bonds will be
 more compressible, and that therefore a positive excess volume will result in a
 negative excess bulk modulus. The reverse is also true; shorter bonds are likely
 to be less compressible. Of course, compression in complex minerals is unlikely
 to be well-described by a simple isotropic change in bond length. Nevertheless,
 30 other compression mechanisms such as polyhedral rotation are likely to be af-
 fected in a similar way; in general, a smaller volume will reduce the flexibility
 of the structure.

Thermoelastic models are also increasingly being used to interpret seismic
 data in terms of the temperature and composition of the deep Earth. Studies
 35 have focussed on Earth’s mantle (e.g. Davies et al., 2012; Mosca et al., 2012;
 Deschamps et al., 2012) and core (e.g. Sanloup et al., 2000, 2004), and with
 the successful deployment of seismometers may soon extend to Mars (Gudkova
 et al., 2014). Again, the bulk modulus imposed by the constant excess volume
 approximation may be a significant and unnecessary contributor to error in these
 40 studies, especially for metallic liquids, where excess volumes at low pressures
 are often very large.

The current study addresses the problems outlined above by adapting the
 subregular Margules mixing model, using intermediate compounds to describe
 the excess properties of the solid solution. The added flexibility comes with
 45 a large increase in the number of free parameters, so useful heuristics are also
 provided to estimate these where independent constraints are unavailable. The
 new formulation should enable a large number of studies on elastic properties
 of solid solutions to be incorporated into thermodynamic models. This study
 also highlights the need for high quality equation of state and seismic velocity
 50 data for intermediate compositions within solid solutions.

2. Theory

2.1. The Extended Subregular Margules (ESM) model

The subregular Margules mixing model within a binary system A - B approximates excess Gibbs free energies at any given pressure and temperature as a cubic function of composition (Helffrich and Wood, 1989):

$$\mathcal{G}^{xs} = X_B(1 - X_B)(W_{AB}X_B + W_{BA}(1 - X_B)) \quad (2)$$

In the special case that $W_{AB} = W_{BA}$, the function is a quadratic. I can define the Gibbs interaction parameter in terms of the Gibbs free energy of a 50:50 intermediate compound (AB) and the endmembers A and B :

$$W_{AB}^{\mathcal{G}} = 4(\mathcal{G}_{AB} + T\mathcal{S}_{AB}^{\text{conf}}) - 2(\mathcal{G}_A + \mathcal{G}_B) \quad (3)$$

where $\mathcal{S}_{AB}^{\text{conf}}$ is the configurational entropy of the intermediate compound. In the more general case that $W_{AB} \neq W_{BA}$, Equation 2 can be thought of as two symmetric interaction parameters with contributions that depend on the composition. Two intermediate compounds (AB and BA) are then required to describe the properties of the solution (Figure 1).

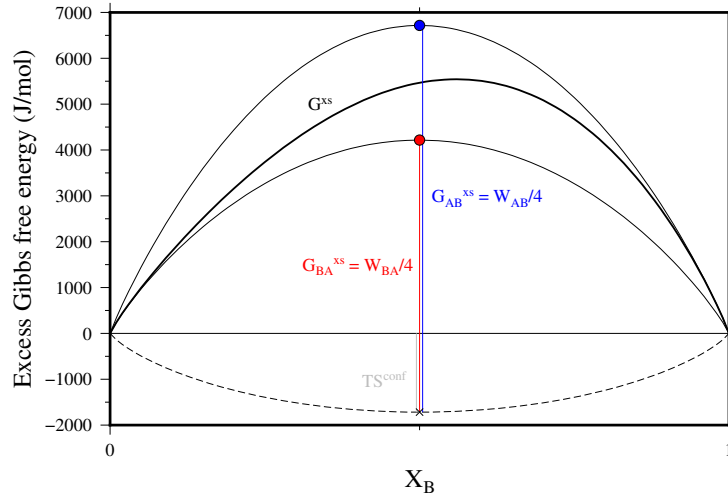


Figure 1: Schematic illustration of excess energies within a binary subregular solution model.

Expanding the subregular solution model beyond a binary system, the excess
 65 nonconfigurational Gibbs free energy is (Helffrich and Wood, 1989)

$$\mathcal{G}^{xs} = \sum_{i=1}^n \sum_{j>1}^n X_i X_j \left(W_{ij} X_j + W_{ji} X_i + 0.5(W_{ij} + W_{ji}) \sum_k^n (1 - \delta_{ik})(1 - \delta_{jk}) X_k \right) \quad (4)$$

Each of the individual W_{ij} terms in Equation 4 can be determined via the properties of an intermediate compound, just as described in the binary A - B system (Equation 2). The properties of the solid solution with composition \mathbf{X} are then defined as follows:

$$\mathcal{G} = \sum_i X_i \mathcal{G}_i + \mathcal{G}^{xs} \quad (5)$$

$$\mathcal{H} = \sum_i X_i \mathcal{H}_i + \mathcal{H}^{xs} \quad (6)$$

$$\mathcal{S} = \sum_i X_i \mathcal{S}_i + \mathcal{S}^{xs} \quad (7)$$

$$\mathcal{V} = \sum_i X_i \mathcal{V}_i + \mathcal{V}^{xs} \quad (8)$$

$$C_P = \sum_i X_i C_P + T \left(\frac{\partial \mathcal{S}}{\partial T} \right)_P^{xs} \quad (9)$$

$$\alpha = \frac{1}{\mathcal{V}} \left(\sum_i X_i \alpha_i \mathcal{V}_i + \left(\frac{\partial \mathcal{V}}{\partial T} \right)_P^{xs} \right) \quad (10)$$

$$K_T = \frac{\mathcal{V}}{\sum_i \frac{X_i \mathcal{V}_i}{K_{Ti}} - \left(\frac{\partial \mathcal{V}}{\partial P} \right)_T^{xs}} \quad (11)$$

$$C_V = C_P - \mathcal{V} T \alpha^2 K_T \quad (12)$$

$$K_S = K_T \frac{C_P}{C_V} \quad (13)$$

$$\gamma = \frac{\alpha K_T \mathcal{V}}{C_V} \quad (14)$$

70 With the exception of the enthalpy excess, excess terms (\mathcal{S}^{xs} , \mathcal{V}^{xs} etc) are derived in the same way as the excess Gibbs free energy (Equation 4), with interaction terms defined as follows:

$$W_{ij}^{\mathcal{S}} = 4(\mathcal{S}_{ij} - \mathcal{S}_{ij}^{\text{conf}}) - 2(\mathcal{S}_i + \mathcal{S}_j) \quad (15)$$

$$W_{ij}^{\mathcal{V}} = 4\mathcal{V}_{ij} - 2(\mathcal{V}_i + \mathcal{V}_j) \quad (16)$$

$$W_{ij}^{\partial\mathcal{V}/\partial P} = -4\mathcal{V}_{ij}/K_{Tij} + 2(\mathcal{V}_i/K_{Ti} + \mathcal{V}_j/K_{Tj}) \quad (17)$$

$$W_{ij}^{\partial\mathcal{V}/\partial T} = 4\alpha_{ij}\mathcal{V}_{ij} - 2(\alpha_i\mathcal{V}_i + \alpha_j\mathcal{V}_j) \quad (18)$$

$$W_{ij}^{\partial\mathcal{S}/\partial T} = \frac{4C_{Pij} - 2(C_{Pi} + C_{Pj})}{T} \quad (19)$$

Finally, excess enthalpy is defined as

$$\mathcal{H}^{xs} = \mathcal{G}^{xs} + T\mathcal{S}^{xs} \quad (20)$$

2.2. Heuristics

75 It is often the case that endmembers are particularly well studied, while the properties of the solid solution are constrained only by enthalpies of solution and volumes at room temperature and pressure. The remaining properties of the intermediate compounds must be estimated by the user. In this study, we suggest that the following heuristics be used:

$$\mathcal{S}_{ij} = 0.5(\mathcal{S}_i + \mathcal{S}_j) + \mathcal{S}_{ij}^{\text{conf}} \quad (21)$$

$$C_{Pij} = 0.5(C_{Pi} + C_{Pj}) \quad (22)$$

$$\alpha_{ij} = 0.5\mathcal{V}\left(\frac{\alpha_i}{\mathcal{V}_i} + \frac{\alpha_j}{\mathcal{V}_j}\right) \quad (23)$$

$$K'_T = -\frac{\partial}{\partial P}\left(\mathcal{V}\left(\frac{\partial P}{\partial \mathcal{V}}\right)_T\right) \sim \mathcal{V}\left(\sum_i \frac{X_i\mathcal{V}_i}{K'_{Ti} + 1}\right)^{-1} - 1 \quad (24)$$

80 If excess volumes are zero, it is likely that they will remain zero as temperatures and pressures increase. In this case, the bulk modulus is given by Equation 11, with the differential term equal to zero. In contrast, non-zero excess volumes are unlikely to remain constant with pressure and temperature. I suggest that, in the absence of other data a useful heuristic is $(\frac{\partial \mathcal{V}}{\partial P})_T^{xs} \rightarrow 0$ as $P \rightarrow \infty$.

85 A useful way to view the change in bulk modulus across a solid solution is to compare the excess bulk modulus to that implied by the $K_TV = \text{constant}$ rule of thumb proposed by Anderson and Anderson (1970) to estimate the compressibility of endmembers based on their molar volumes. The heuristic we propose in this study predicts a larger excess term than that suggested by the rule of thumb, which we describe using a factor ξ :

90

$$K_T \sim 0.5(K_{Ti} + K_{Tj}) + \xi \left(\frac{K_{Ti}\mathcal{V}_j + K_{Tj}\mathcal{V}_i}{2\mathcal{V}} - 0.5(K_{Ti} + K_{Tj}) \right) \quad (25)$$

Typically, a value of ~ 6 provides a useful estimate of ξ .

Now that we have described the new model and heuristics related to the construction of intermediate compounds, we turn to a few geologically relevant examples. The models in this study are all implemented in the open software *burnman*, a mineral physics toolkit written in python. The software, first described in Cottaar et al. (2014), was originally designed for seismic velocity calculations. It has since been augmented with thermodynamics functionality, including a range of different models for solid solutions.

3. Examples

3.1. Pyroxene

Our first example is that of jadeite-aegirine pyroxene, an almost ideal solid solution (from a volumetric perspective). I use this model to illustrate that even when excess volumes are extremely small, excess bulk moduli are resolvable. The experimental data is that of Nestola et al. (2006), and the equation of state used is the Modified Tait (Holland and Powell, 2011). The fit to the volume data is shown in Figure 2.

Table 1: Jadeite-Aegirine mixing parameters to fit the room temperature data of Nestola et al. (2006). The K'_0 for the intermediate compound is fixed to the value given by the heuristic proposed in the text. $K''_0 = -K'_0/K_0$.

	jadeite	aegirine	jd ₅₀ ae ₅₀	ae ₅₀ jd ₅₀
V_0 (cm ³ /mol)	60.5640 ± 0.0001	64.6261 ± 0.0004	62.3641 ± 0.0005	62.4522 ± 0.0005
K_0 (GPa)	133.5 ± 0.2	116.0 ± 0.2	124.8 ± 0.5	126.7 ± 0.4
K'_0	4.6 [fixed]	4.4 [fixed]	4.4785 [heuristic]	4.4785 [fixed]

Using the derived properties of the solid solution, we can fit the excess volume as a function of pressure (Figure 3). The decay of excess volume as a function

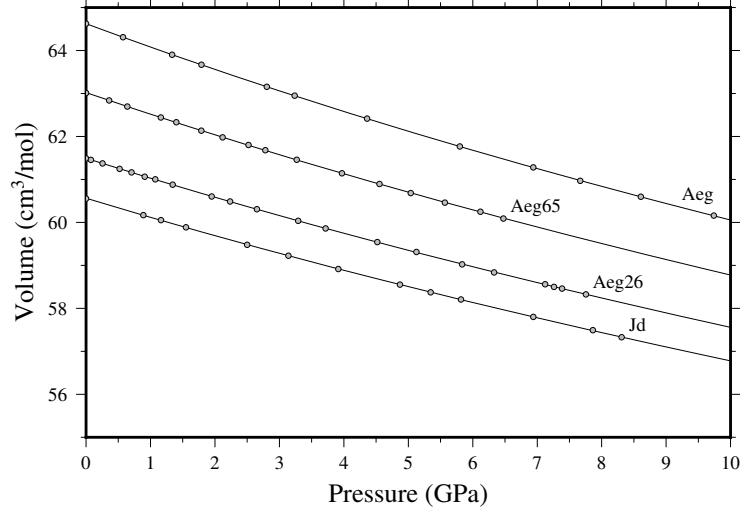


Figure 2: Pressure-volume data in the binary system jadeite-aegirine (Nestola et al., 2006). Solid lines correspond to the volumes predicted by the model proposed in this study.

of pressure is in excellent agreement with the prediction that excess volumes
 110 decay to zero at extreme pressures. For the 50:50 intermediate, our excess bulk
 moduli and volumes indicate that $\xi \sim 11$ (Equation 25).

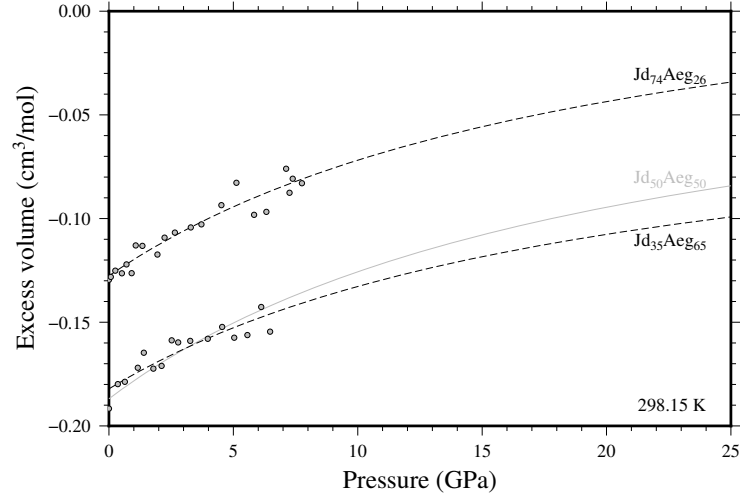


Figure 3: Excess volume for jadeite-aegirine pyroxenes (Nestola et al., 2006). Solid lines correspond to the modelled excess volumes.

3.2. Garnet

Our first example dealt with a solid solution which has small excess volumes, but some phases exhibit significantly larger excesses. One example is the
115 garnet system. Of particular interest is the pyrope-grossular join. Grossular is a major secondary component of many natural pyrope garnets. The size mismatch between the small magnesium cation and the large calcium cation on the dodecahedral site results in a large positive excess volume (Newton et al., 1977; Bosenick and Geiger, 1997; Ganguly et al., 1996). Recently, it has been
120 suggested that the excess volumes of mixing are $\sim 1 \text{ cm}^3/\text{mol}$, 2–3 times larger than previously considered, and associated with very large negative excess bulk moduli (Du et al., 2015). It is proposed that the differences are due to a hydrogrossular component in the crystals synthesised in piston cylinder apparatus in earlier studies, which becomes unstable at high pressures. Such a large varia-
125 tion in bulk modulus would have a major impact on seismic velocities and excess properties at high pressure. Since garnets remain stable to the uppermost lower mantle, a careful analysis of these effects is warranted.

Here, we create four models to describe the room temperature equations of state for the pyrope-grossular system using the pyrope and grossular endmembers from Holland and Powell (2011). Two models are presented for the data
130 of (Du et al., 2015), to describe the reported behaviour close to the center and at the edges of the solid solution. The third model is the constant volume sub-regular Margules model of Ganguly et al. (1996). A fourth model has the same excess volume as Ganguly et al. (1996), but a negative excess bulk modulus
135 which allows the excess volume to decay to zero at high pressures ($\xi = 6$). The standard state bulk moduli are shown in Figure 4.

It is immediately obvious that the bulk moduli calculated from the Du et al. (2015) study exhibit very large deviations from a linear trend. The symmetric curve derived from the two compounds in the middle of the binary yields $\xi = 10$,
140 a value which is not unreasonable, and results in a change in sign of the volume excess at 20–25 GPa. In contrast, the trend derived from the compounds with 20% and 80% pyrope content yields $\xi = 52$. This extreme value leads to negative

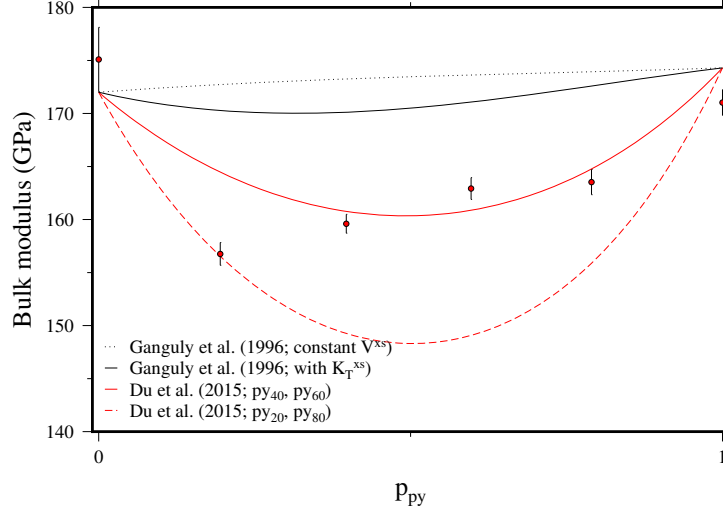


Figure 4: Bulk moduli in the pyrope-grossular binary. Data points are those reported by Du et al. (2015). The four models correspond to those discussed in the main text.

excess volumes at 5–6 GPa, which does not seem to be very likely. To avoid this, K_T' must be increased to >20 , which is also extremely unlikely.

145 The trend calculated from the terms in Ganguly et al. (1996) has a small positive excess bulk modulus, which is always the case where \mathcal{V}^{xs} is held fixed. For the reasons outlined in the introduction, this is probably unlikely. The final model, constructed using the heuristics described in the previous section yields an excess bulk modulus on the order of 2–3 GPa.

150 These models are now used to illustrate the effect of different excess volume models on seismic wave velocities. P-wave, S-wave and bulk sound velocities are functions of isentropic bulk and shear moduli and density:

$$V_P = \sqrt{\frac{K_S + \frac{4}{3}G}{\rho}} \quad (26)$$

$$V_S = \sqrt{\frac{G}{\rho}} \quad (27)$$

$$V_\Phi = \sqrt{\frac{K_S}{\rho}} \quad (28)$$

Thermodynamic solution models say nothing about shear moduli, so we restrict

our discussion to the bulk sound velocity. Figure 5 shows the bulk sound velocity
 155 at ambient temperature for the four solid solution models in the text. The
 models of Du et al. (2015) result in large depressions of bulk sound velocity. The
 model constructed from the py₄₀ and py₆₀ samples results in a 4% depression
 relative to the constant V^{xs} case throughout the upper mantle pressure range.
 In contrast, the model based on the excess volume model proposed in Ganguly
 160 et al. (1996) predicts a 1% decrease in bulk sound speed.

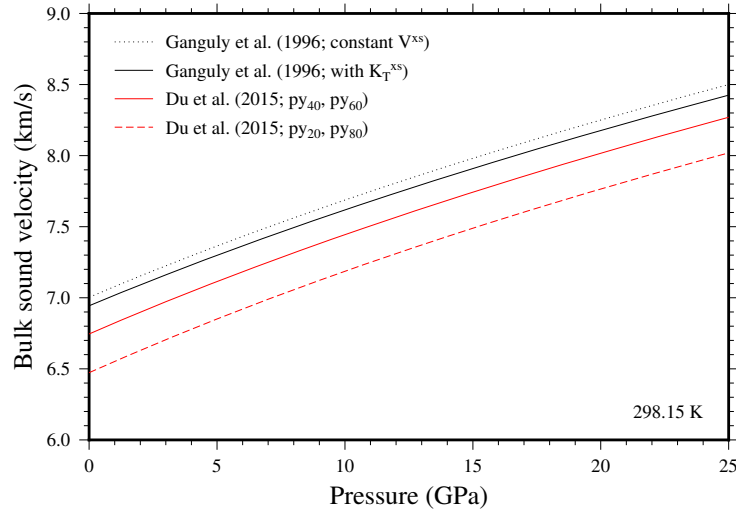


Figure 5: Bulk sound velocities of py₅₀gr₅₀ at room temperature according to the models described in the text and in Figure 4.

It is not yet clear whether natural garnets have P-V-T equations of state
 similar to those suggested by Du et al. (2015), or similar to those in previous
 studies (Newton et al., 1977; Bosenick and Geiger, 1997; Ganguly et al., 1996).
 If a hydrogrossular component is indeed the cause for low excess volumes in
 165 piston cylinder-synthesised garnets, then garnets in the mantle are likely to have
 relatively high volume excesses and low bulk moduli. In this case, constant V^{xs}
 models are clearly inappropriate both for calculations of mantle phase relations
 and seismic velocities. Even in the case of the model derived from Ganguly et al.
 (1996), the difference in free energy compared with the constant V^{xs} model is

170 on the order of kilojoules at the bottom of the mantle transition zone.

The heuristics suggested here place constraints on seismic properties which are significantly more strict than typical uncertainties on bulk moduli derived from ultrasonic interferometry, Brillouin scattering or static compression. For example, along the pyrope-majorite join, excess volumes are small ($0.1 \text{ cm}^3/\text{mol}$)
175 (Heinemann et al., 1997). With the assumption that excess volumes decrease to zero with increasing pressure, the excess bulk modulus is constrained to be ~ 0.6 GPa. In comparison, the range in bulk modulus estimates anywhere along the pyrope-majorite join is about 10 GPa (see, for example Hunt et al., 2010). So far, high pressure elasticity studies have mostly been focussed on binary joins
180 with small excess volumes at ambient pressure (Fan et al., 2015; Huang and Chen, 2014). That they should exhibit small excess bulk moduli is in excellent agreement with the heuristics proposed here, but a far more rigorous test would be to investigate systems with large volume excesses.

3.3. *Metallic-ionic melt*

185 The thermodynamics and thermoelastics of ionic and metallic melts is fundamental to our understanding of core differentiation. During the formation of the terrestrial planets, it is thought that oligarchic growth led to a series of mixed silicate-metallic magma oceans, from which metallic melts separated before sinking as diapirs into the growing core (Rubie et al., 2015). Although these
190 melts are predominantly composed of iron and nickel, several weight percent of light elements are required to explain the Earth’s density deficit and low seismic velocities (Poirier, 1994). These light elements not only influence the melting point of the core (which directly informs us about the temperature of the inner core boundary), but also the style of crystallisation, and therefore the generation
195 of a magnetic dynamo (Stewart et al., 2007). Since equilibration with a magma ocean governs the initial composition of the core, and seismology presents us with the most direct information on the present composition of the core, accurate thermodynamic modelling is vitally important to our understanding of the evolution and present chemical state of the Earth. It is well known that

several iron-light element binaries are associated with large non-idealities (e.g. Frost et al., 2010), so accurate modelling requires changes in excess properties in these systems to be taken into account.

Oxygen is a good example of a light element which exhibits a large degree of non-ideality. At pressures <25 GPa, the Fe-FeO solution exhibits significant non-ideality, with a large miscibility gap between ionic and metallic Fe-O liquids (Kowalski and Spencer, 1995; Tsuno et al., 2007; Frost et al., 2010). As pressure increases, this miscibility gap disappears, indicating a negative excess volume of mixing (Figure 6).

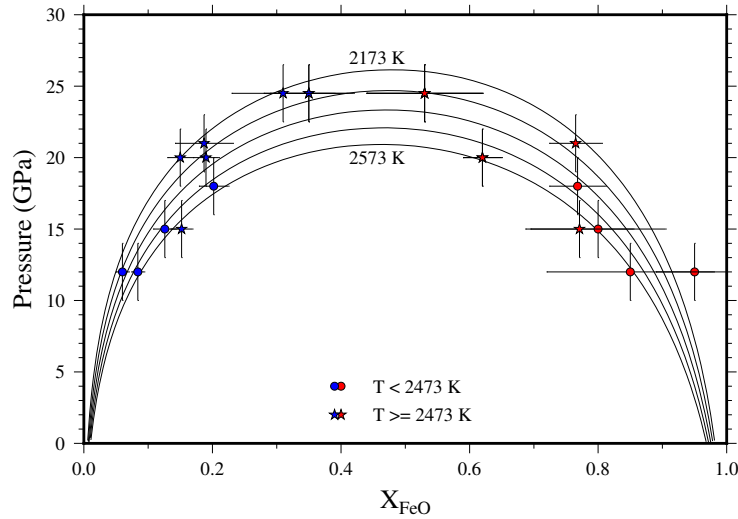


Figure 6: The Fe-FeO solvus as a function of pressure and temperature. Data points are taken from the studies of Tsuno et al. (2007) and Frost et al. (2010). The model corresponds to the values proposed in Table 2.

To constrain the properties of the Fe-FeO solid solution, the chemical potentials of Fe and FeO are estimated from the compositions of coexisting ionic and metallic melts at <25 GPa, and the pressure, temperature and compositions of eutectic liquid at >25 GPa (Seagle et al., 2008). The latter constraints also require thermodynamic data for the eutectic phases (B1-structured FeO and FCC and HCP iron), which are calculated from room pressure data and constraints on the melting curves (Seagle et al., 2008; Ozawa et al., 2011; Anzellini et al.,

2013; Komabayashi, 2014). The Margules parameters estimated from this data are shown in Figure 7.

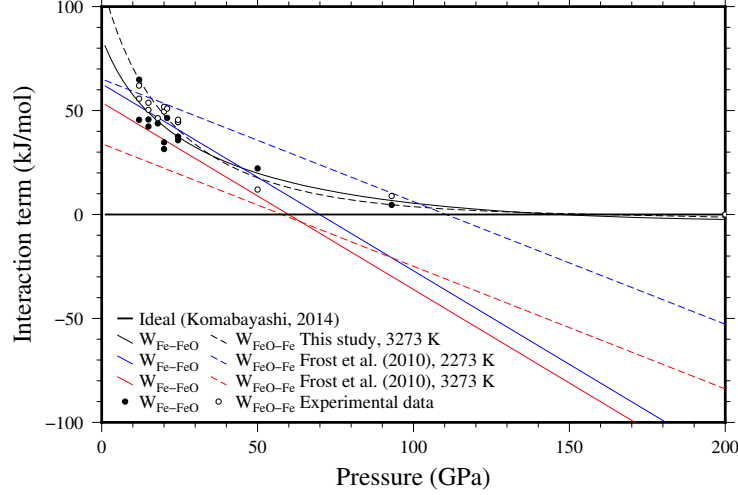


Figure 7: Interaction terms in Fe-FeO melt as a function of pressure. Experimental data comes from solvus constraints at <25 GPa (Tsuno et al., 2007; Frost et al., 2010), and the composition and temperature of the eutectic at higher pressures (Seagle et al., 2008).

The uncertainties on composition and temperature of the eutectic are rather large, so these data are supplemented by the requirement that excess volumes become zero at very high pressure. The parameters used to create the fits in Figures 7 and 8 are given in Table 2. It is assumed that excess entropy and thermal expansion are negligible. The majority of the <25 GPa data was collected within a ~ 200 K temperature range, and is associated with similar temperature uncertainties, which introduces very large uncertainties in excess entropies. Add to that the possibility of phase separation during quench and the large uncertainty in coexisting ionic/metallic melt compositions, there is no clear evidence for the large temperature dependence proposed by Frost et al. (2010), although they do slightly improve the fit to the data (mostly by increasing the pressure at which the solvus closes at high temperature).

The constant negative volume excesses in the model of Frost et al. (2010) produce reasonable eutectic melting temperatures up to ~ 50 GPa. Beyond

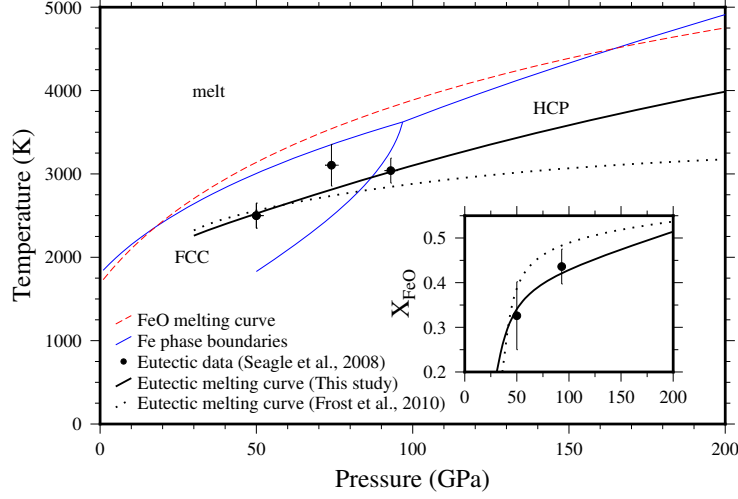


Figure 8: Melting temperature in the Fe-O system as a function of pressure. Inset: eutectic composition in the Fe-O system. Data points are from Seagle et al. (2008). The model of Frost et al. (2010) employs constant volume and entropy terms derives from data obtained at <25 GPa, and deviates significantly from experimental constraints at pressures corresponding to the Earth’s core.

Table 2: Excess Fe-FeO mixing parameters to fit the data in Figures 7 and 8 at a reference temperature of 1809 K and pressure of 50 GPa.

Property	Fe ₅₀ FeO ₅₀	FeO ₅₀ Fe ₅₀
H^{xs} (J/mol)	5000 ± 400	4400 ± 400
S^{xs} (J/K/mol)	0 [fixed]	0 [fixed]
V^{xs} (cm ³ /mol)	-0.117 ± 0.009	-0.136 ± 0.009
K^{xs} (GPa)	28 ± 5	45 ± 5
K'^{xs}	-0.07 ± 0.12	-0.37 ± 0.12
a^{xs}	0 [fixed]	0 [fixed]

235 this point, the increasing pressure stabilisation of the solution results in large deviations from the slope of the melting curve (Figure 8). This effect becomes very large at inner core boundary pressures (330 GPa), where solid Fe and FeO are stable to at least ~ 4200 K (Ozawa et al., 2011). In contrast, the melting point derived from the parameters of Frost et al. (2010) reaches a maximum at

3225 K and 275 GPa. The best fit excess bulk moduli in Table 2 are large, even at the reference pressure of 50 GPa. Such values will have a significant effect on seismic velocities, especially at the pressures corresponding to the cores of small planetary bodies.

4. Discussion

The use of intermediate compounds to describe excess properties within the framework of simple solution models lends the flexibility required to create single thermoelastodynamic models covering very large P - T ranges. In this study, the high pressure properties of pyroxenes, garnets and melts are used to illustrate the development of such models, and their ability to accurately reproduce observed variations in pressure, temperature or compositional derivatives of the Gibbs free energy, such as bulk modulus and chemical potentials. Without these, it would be impossible to accurately model phase relations at extreme conditions, or seismic velocities.

This study does not discuss the behaviour of the shear modulus across solid solutions. Thermodynamic databases are now starting to include shear moduli and their change with pressure and temperature (Stixrude and Lithgow-Bertelloni, 2011), so constraining these changes across solid solutions should also be a key priority for experimental and ab-initio studies. Using intermediate compounds to describe the change in shear modulus across a solid solution should work well, especially in silicate systems, where excess shear moduli may be of similar magnitude to excess bulk moduli, and also decrease with increasing pressure (e.g Lacivita et al., 2014).

The heuristics suggested in this study agree with the available data on the three example systems, but remain heuristics only. It would be particularly interesting to investigate the change in excess volumes with temperature and pressure for other systems in which excess properties are large, and interpret these in terms of crystal or melt structures. Conversely, the behaviour of systems with small excesses at room temperature and pressure should also be investi-

gated. Current evidence suggests that small volume excesses at low pressure remain small under different conditions (Fan et al., 2015; Huang and Chen, 2014), but this may not be true for all solutions.

In the case of ionic and metallic melts, excess volumes can be extremely large
270 at low pressure. The large excess elastic moduli accompanying these excess
volumes will have a large effect on seismic velocities, especially in the cores
of relatively small bodies such as Mars or the Moon. As pressures increase,
excess volumes are much reduced, which has a similarly profound effect on
thermodynamic properties (Frost et al., 2010; de Koker et al., 2013). Accurate
275 characterisation of excess properties of melt solutions, and indeed of solutions
in general, will become increasingly important for our interpretation of seismic
anomalies, modelling of phase relations, and our understanding of planetary
evolution.

5. Acknowledgments

280 RM is funded by the Advanced ERC Grant awarded to the “ACCRETE”
project (Contract number 290568). He would like to thank Dave Rubie, Dan
Frost and Christopher Beyer for useful discussions.

References

- Anderson, D.L., Anderson, O.L., 1970. Brief report: The bulk modulus-volume
285 relationship for oxides. *Journal of Geophysical Research* 75, 3494–3500.
- Anzellini, S., Dewaele, A., Mezouar, M., Loubeyre, P., Morard, G., 2013. Melt-
ing of Iron at Earth’s Inner Core Boundary Based on Fast X-ray Diffraction.
Science 340, 464–466.
- Bosenick, A., Geiger, C.A., 1997. Powder x ray diffraction study of synthetic
290 pyrope-grossular garnets between 20 and 295 k. *Journal of Geophysical Re-
search: Solid Earth* 102, 22649–22657.
- Cottaar, S., Heister, T., Rose, I., Unterborn, C., 2014. BurnMan: A lower
mantle mineral physics toolkit. *Geochemistry, Geophysics, Geosystems* 15,
1164–1179.
- 295 Davies, D.R., Goes, S., Davies, J., Schuberth, B., Bunge, H.P., Ritsema, J.,
2012. Reconciling dynamic and seismic models of earth’s lower mantle: The
dominant role of thermal heterogeneity. *Earth and Planetary Science Letters*
353-354, 253 – 269.
- de Koker, N., Karki, B.B., Stixrude, L., 2013. Thermodynamics of the MgO-
300 SiO₂ liquid system in Earth’s lowermost mantle from first principles. *Earth
and Planetary Science Letters* 361, 58–63.
- Deschamps, F., Cobden, L., Tackley, P.J., 2012. The primitive nature of
large low shear-wave velocity provinces. *Earth and Planetary Science Let-
ters* 349350, 198 – 208.
- 305 Du, W., Clark, S.M., Walker, D., 2015. Thermo-compression of pyrope-grossular
garnet solid solutions: Non-linear compositional dependence. *American Min-
eralogist* 100, 215–222.
- Fan, D., Xu, J., Ma, M., Liu, J., Xie, H., 2015. Pvt equation of state of
spessartinealmandine solid solution measured using a diamond anvil cell and

- 310 in situ synchrotron x-ray diffraction. *Physics and Chemistry of Minerals* 42,
63–72.
- Frost, D.J., Asahara, Y., Rubie, D.C., Miyajima, N., Dubrovinsky, L.S.,
Holzapfel, C., Ohtani, E., Miyahara, M., Sakai, T., 2010. Partitioning of
oxygen between the Earth’s mantle and core. *Journal of Geophysical Re-*
315 *search (Solid Earth)* 115, 2202.
- Ganguly, J., Cheng, W., Tirone, M., 1996. Thermodynamics of aluminosili-
cate garnet solid solution: new experimental data, an optimized model, and
thermometric applications. *Contributions to Mineralogy and Petrology* 126,
137–151.
- 320 Gudkova, T., Lognonné, P., Zharkov, V., Raevsky, S., 2014. On the scientific
aims of the miss seismic experiment. *Solar System Research* 48, 11–21.
- Heinemann, S., Sharp, T.G., Seifert, F., Rubie, D.C., 1997. The cubic-
tetragonal phase transition in the system majorite ($\text{Mg}_4\text{Si}_4\text{O}_{12}$) - pyrope
($\text{Mg}_3\text{Al}_2\text{Si}_3\text{O}_{12}$), and garnet symmetry in the Earth’s transition zone. *Physics*
325 *and Chemistry of Minerals* 24, 206–221.
- Helfrich, G., Wood, B.J., 1989. Subregular model for multicomponent solutions.
American Mineralogist 74, 1016–1022.
- Holland, T.J., Hudson, N.F., Powell, R., Harte, B., 2013. New thermodynamic
models and calculated phase equilibria in ncfmas for basic and ultrabasic
330 compositions through the transition zone into the uppermost lower mantle.
Journal of Petrology 54, 1901–1920.
- Holland, T.J.B., Powell, R., 2011. An improved and extended internally con-
sistent thermodynamic dataset for phases of petrological interest, involving a
new equation of state for solids. *Journal of Metamorphic Geology* 29, 333–383.
- 335 Huang, S., Chen, J., 2014. Equation of state of pyrope-almandine solid solution
measured using a diamond anvil cell and in situ synchrotron X-ray diffraction.
Physics of the Earth and Planetary Interiors 228, 88–91.

- Hunt, S.A., Dobson, D.P., Li, L., Weidner, D.J., Brodholt, J.P., 2010. Relative strength of the pyropemajorite solid solution and the flow-law of majorite containing garnets. *Physics of the Earth and Planetary Interiors* 179, 87 – 95.
- Komabayashi, T., 2014. Thermodynamics of melting relations in the system Fe-FeO at high pressure: Implications for oxygen in the Earth’s core. *Journal of Geophysical Research (Solid Earth)* 119, 4164–4177.
- 345 Kowalski, M., Spencer, P., 1995. Thermodynamic reevaluation of the C-O, Fe-O and Ni-O systems: Remodelling of the liquid, BCC and FCC phases. *Calphad* 19, 229 – 243.
- Lacivita, V., Erba, A., Dovesi, R., D’Arco, P., 2014. Elasticity of grossular-andradite solid solution: an ab initio investigation. *Phys. Chem. Chem. Phys.* 16, 15331–15338.
- 350 Mosca, I., Cobden, L., Deuss, A., Ritsema, J., Trampert, J., 2012. Seismic and mineralogical structures of the lower mantle from probabilistic tomography. *Journal of Geophysical Research: Solid Earth* 117. B06304.
- Nestola, F., Boffa Ballaran, T., Liebske, C., Bruno, M., Tribaudino, M., 2006. High-pressure behaviour along the jadeite NaAlSi₂O₆-aegirine NaFeSi₂O₆ solid solution up to 10 GPa. *Physics and Chemistry of Minerals* 33, 417–425.
- 355 Newton, R.C., Charlu, T.V., Kleppa, O.J., 1977. Thermochemistry of high pressure garnets and clinopyroxenes in the system CaO-MgO-Al₂O₃-SiO₂. *Geochimica et Cosmochimica Acta* 41, 369–377.
- 360 Ozawa, H., Takahashi, F., Hirose, K., Ohishi, Y., Hirao, N., 2011. Phase Transition of FeO and Stratification in Earth’s Outer Core. *Science* 334, 792–.
- Poirier, J.P., 1994. Light elements in the earth’s outer core: A critical review. *Physics of the Earth and Planetary Interiors* 85, 319 – 337.

- 365 Rubie, D., Jacobson, S., Morbidelli, A., O'Brien, D., Young, E., de Vries, J.,
Nimmo, F., Palme, H., Frost, D., 2015. Accretion and differentiation of the
terrestrial planets with implications for the compositions of early-formed solar
system bodies and accretion of water. *Icarus* 248, 89 – 108.
- Sanloup, C., Fiquet, G., Gregoryanz, E., Morard, G., Mezouar, M., 2004. Effect
370 of Si on liquid Fe compressibility: Implications for sound velocity in core
materials. *Geophysical Research Letters* 31, 7604.
- Sanloup, C., Guyot, F., Gillet, P., Fiquet, G., Mezouar, M., Martinez, I., 2000.
Density measurements of liquid Fe-S alloys at high-pressure. *Geophysical
Research Letters* 27, 811–814.
- 375 Seagle, C.T., Heinz, D.L., Campbell, A.J., Prakapenka, V.B., Wanless, S.T.,
2008. Melting and thermal expansion in the Fe-FeO system at high pressure.
Earth and Planetary Science Letters 265, 655–665.
- Stewart, A.J., Schmidt, M.W., van Westrenen, W., Liebske, C., 2007. Mars: A
new core-crystallization regime. *Science* 316, 1323–1325.
- 380 Stixrude, L., Lithgow-Bertelloni, C., 2011. Thermodynamics of mantle minerals
- II. Phase equilibria. *Geophysical Journal International* 184, 1180–1213.
- Tsuno, K., Ohtani, E., Terasaki, H., 2007. Immiscible two-liquid regions in the
Fe–O–S system at high pressure: Implications for planetary cores. *Physics of
the Earth and Planetary Interiors* 160, 75–85.